A Theoretical Model for Magneto-Acoustic Imaging of Bioelectric Currents

Bradley J. Roth, Peter J. Basser, and John P. Wikswo, Jr.

Abstract— **A theoretical model of magneto-acoustic current imaging is derived, based on fundamental equations of continuum mechanics and electromagnetism. In electrically active tissue, the interaction between an applied magnetic field, B, and action currents, J, creates a pressure distribution. In the near field limit, this pressure obeys Poisson's equation, with a source term $(\nabla \times J) \cdot B$. The displacement and pressure fields are calculated for a dipole (q), oriented either parallel or perpendicular to the applied magnetic field (B), at the center of an elastic, conducting sphere (radius a, shear modulus G). Surface displacements are on the order of $qB/(4\pi Ga)$, which is about 1 nm for typical biological parameters. If the applied magnetic field is changing with time, eddy currents induced in the tissue may be larger than the action currents themselves. The frequency of the pressure and displacement arising from these eddy currents, however, is twice the frequency of the applied magnetic field, so it may be possible to eliminate this artifact by filtering or lock-in techniques. Magneto-acoustic and biomagnetic measurements both image $\nabla \times J$ in a similar way, although magneto-acoustic current imaging has the disadvantage that acoustic properties vary among tissues to a greater degree than do magnetic properties.**

I. Introduction

RECENTLY, a magneto-acoustic technique has been developed to image electrical current in biological tissue [1]–[4]. In the presence of an externally applied magnetic field, B, bioelectric action currents, J, arising from active nerve or muscle fibers, experience a Lorentz force [5], $J \times B$. The resulting pressure or tissue displacement contains information about the action currents. This technique has been used to detect microampere-level currents introduced into hamsters [1], and has been suggested as a method for reconstructing images of current dipoles [2] and for imaging action currents produced by a single nerve [3]. In this paper, we provide the mathematical basis for magneto-acoustic current imaging using the fundamental equations of continuum mechanics and electromagnetism, and assess the capabilities and limitations of magneto-acoustic current imaging as a technique to analyze bioelectric currents *in vitro* and *in vivo*.

Our model is predicated on three assumptions. 1) The applied magnetic field, B, is much larger than the biomagnetic field, b, produced by the bioelectric action currents. The biomagnetic field 1 mm from an active frog sciatic nerve is about 100 pT [6], whereas the magnetic field applied during magneto-acoustic imaging is 10 to 100 mT [1], implying that the endogenous and applied magnetic field strengths differ by a factor of at least 10^8. 2) The bioelectric current is not affected by the applied magnetic field. The Lorentz force is small compared to the electrical force producing the action currents; a steady magnetic field of 24 T is required to produce a 10% change in the action currents [7]. Magneto-acoustic imaging uses field strengths of about 100 mT, so perturbations of action current distributions by the applied magnetic field are approximately 0.1%. 3) The action currents vary slowly enough in time that the displacement (capacitive) currents[1] and effects from the propagation of electromagnetic radiation are negligible (quasistationarity) [9]. If the applied magnetic field is changing with time, we make one additional assumption. 4) The size of the tissue sample is much smaller than the skin depth [5]. At 1 kHz, which is the highest frequency typically encountered during magneto-acoustic imaging [1], [4], the skin depth is 16 m in a tissue with a conductivity of 1 S/m.

Manuscript received May 4, 1993; revised February 16, 1994.

B. J. Roth and P. J. Basser are with the Biomedical Engineering and Instrumentation Program, National Center for Research Resources, National Institutes of Health, Bethesda, MD 20892 USA.

J. P. Wikswo, Jr. is with The Living State Physics Group, Department of Physics and Astronomy, Vanderbilt University, Nashville, TN 37235 USA.

IEEE Log Number 9402539.

II. The Governing Equations

We consider an unbounded, elastic, conducting tissue having homogeneous, isotropic acoustic properties, in which the strains are small enough that the linear theory of elasticity is valid. Navier's equation governs the displacement, u, of the tissue [10],

$$\rho \frac{\partial^2 u}{\partial t^2} = G\nabla^2 u + \frac{G}{1-2\nu}\nabla(\nabla \cdot u) + J \times B \qquad (1)$$

where G, ν, and ρ are the shear modulus, Poisson's ratio, and density of the tissue, and $J \times B$ is the Lorentz force per unit volume[2] [5]. We assume that the material is incompressible ($\nabla \cdot u = 0$ and $\nu = 1/2$) [11], in which case the second term of

[1] Although capacitive currents are appreciable within the cell membrane, the volume of the thin membrane is so small compared to the volume of the resistive intracellular and extracellular media that capacitive currents made an insignificant contribution to either the total Lorentz force or biomagnetic field [8].

[2] As an alternative to the Lorentz force term ($J \times B$) in (1), we could have included a term containing the divergence of the Maxwell stress tensor, T_{ij}, where

$$T_{ij} = \frac{1}{\mu_0}\left[B_i B_j - \frac{1}{2}\delta_{ij}\sum_{k=1}^{3} B_k B_k\right],$$

and B_i is the ith component of the total magnetic field (applied plus biomagnetic). In such an approach, however, we could not neglect the biomagnetic field produced by the action currents relative to the applied magnetic field, since the biomagnetic field supplies the spatial variation that is required for a nonzero divergence of the stress tensor. For this reason, we prefer including the Lorentz force term explicitly.

0018–9294/94$04.00

(1) can be replaced by a hydrostatic pressure-like term, $-\nabla p$, where $p = -G/(1-2\nu)\nabla \cdot \boldsymbol{u}$ in the limit as ν approaches 1/2. We also assume that the tissue is in steady-state (i.e., acoustically quasistatic), so that the acceleration on the left side of (1) is zero. This assumption is valid if the wavelength of the acoustic wave is much larger than the size of the tissue. In tissue, the velocity of sound is about 1500 m/s [12]. Action currents typically vary over periods of about a millisecond, so the wavelength of the associated acoustic wave is about a meter. For distances from the action currents that are much smaller than this, acoustic propagation effects can be ignored. In this near field limit, Navier's equation becomes

$$G\nabla^2 \boldsymbol{u} - \nabla p + \boldsymbol{J} \times \boldsymbol{B} = 0. \tag{2}$$

We can gain additional physical insight by taking the divergence or curl of (2). If first we take the divergence, use the vector calculus identity [5]

$$\nabla \cdot (\boldsymbol{J} \times \boldsymbol{B}) = (\nabla \times \boldsymbol{B}) \cdot \boldsymbol{J} - (\nabla \times \boldsymbol{J}) \cdot \boldsymbol{B}, \tag{3}$$

and assume that the currents producing the applied magnetic field are outside of the body (so that $\nabla \times \boldsymbol{B}$ is zero within the body), we obtain

$$\nabla^2 p = -(\nabla \times \boldsymbol{J}) \cdot \boldsymbol{B}. \tag{4}$$

The pressure obeys Poisson's equation, with a source term that depends on the divergence of the Lorentz force, or equivalently the curl of the action current.

If we take the curl of (2) and use the vector identity [5]

$$\begin{aligned} \nabla \times (\boldsymbol{J} \times \boldsymbol{B}) = &(\nabla \cdot \boldsymbol{B})\boldsymbol{J} - (\nabla \cdot \boldsymbol{J})\boldsymbol{B} \\ &+ (\boldsymbol{B} \cdot \nabla)\boldsymbol{J} - (\boldsymbol{J} \cdot \nabla)\boldsymbol{B} \end{aligned} \tag{5}$$

($\nabla \cdot \boldsymbol{B}$ is zero for all magnetic fields, and $\nabla \cdot \boldsymbol{J}$ is zero under the quasistatic assumption), we obtain

$$2G\nabla^2 \boldsymbol{\omega} = (\boldsymbol{B} \cdot \nabla)\boldsymbol{J} - (\boldsymbol{J} \cdot \nabla)\boldsymbol{B} \tag{6}$$

where $\boldsymbol{\omega}$ is the rotation vector ($2\boldsymbol{\omega} = \nabla \times \boldsymbol{u}$). If $\boldsymbol{B}$ is uniform, only the first term on the right side of (6) is nonzero, and we find that gradients in $\boldsymbol{J}$ that are parallel to $\boldsymbol{B}$ result in shear strains.

III. A Dipole Centered in an Elastic, Conducting Sphere

Our analysis so far has been limited to unbounded media. The displacement and pressure fields, however, are significantly affected by the acoustic boundary conditions at the tissue–air interface, where the pressure must vanish. Thus, we cannot base magneto-acoustic imaging on pressure measurements made over a free surface. Instead, the surface would have to be fixed, or displacement on a free surface must be measured.

One way to appreciate the effect of a surface on the displacement and pressure fields during magneto-acoustic imaging is to consider an elementary example: a current dipole (of strength q) at the center of a sphere (of radius a) in the presence of a uniform magnetic field (of strength B). If we align the dipole along the z-direction, the current density (Fig. 1(a)) is

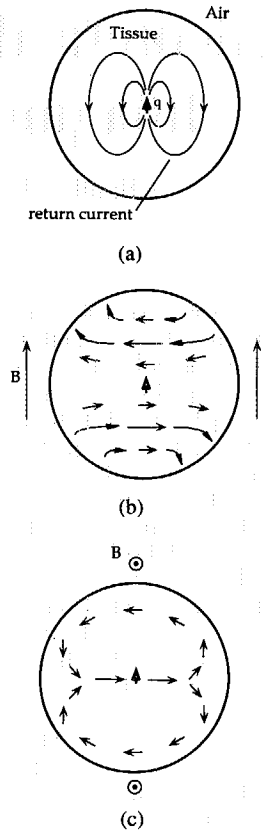

Fig. 1. (a) The current distribution produced by a dipole, q, at the center of a conducting sphere. In (b) and (c), the surface displacements of the sphere are indicated schematically, for the cases when the magnetic field is (b) parallel, and (c) perpendicular to the dipole.

$$\begin{aligned} \boldsymbol{J} = \frac{q}{4\pi a^3}\Bigg[&-2\cos\theta\left(1-\frac{a^3}{r^3}\right)\hat{\boldsymbol{r}} \\ &+ \sin\theta\left(2+\frac{a^3}{r^3}\right)\hat{\boldsymbol{\theta}}\Bigg] \end{aligned} \tag{7}$$

where $\hat{\boldsymbol{r}}$ and $\hat{\boldsymbol{\theta}}$ are unit vectors in the radial and azimuthal directions. At $r = a$ the radial component of the current is zero, as it must be since the air outside the sphere is assumed to be an insulator.

The Lorentz force distribution depends on both $\boldsymbol{J}$ and the direction of the applied magnetic field. When the magnetic field is aligned in the z-direction (parallel to the dipole), the Lorentz force is

$$\boldsymbol{J} \times \boldsymbol{B} = -\frac{3qB}{4\pi r^3}\cos\theta \sin\theta \hat{\boldsymbol{\phi}} \tag{8}$$

where $\hat{\boldsymbol{\phi}}$ is the unit vector in the ϕ-direction. There is no force on the dipole itself because it is parallel to the magnetic field; the force arises entirely from the Ohmic return currents. The net force on the system (dipole plus sphere), integrated over the sphere volume, is zero. The solution to Navier's equation, given the body force in (8) and the constraint that $\nabla \cdot \boldsymbol{u} = 0$, is

$$\boldsymbol{u} = -\frac{qB}{8\pi G r}\cos\theta \sin\theta\, \hat{\boldsymbol{\phi}} \tag{9}$$

$$p = 0. \tag{10}$$

The displacement field is shown schematically in Fig. 1(b). The radial displacement and pressure vanish everywhere, and in particular at the sphere surface. The presence of this dipole, therefore, could be detected only by measurements of the displacement tangent to the sphere surface. The displacements are largest deep in the sphere, and smallest at the surface. Because the torques in the upper hemisphere are opposite to those in the lower hemisphere, there is no net torque on the sphere. The strain is all shear.

When the magnetic field is aligned in the x-direction (perpendicular to the dipole), the body force is

$$\boldsymbol{J}\times\boldsymbol{B}=\frac{3qB}{4\pi a^3}\left\{\left[-\frac{2}{3}-\frac{1}{3}\left(\frac{a}{r}\right)^3(1-3\cos^2\theta)\right]\hat{\boldsymbol{y}}-\left(\frac{a}{r}\right)^3\cos\theta\sin\theta\sin\phi\,\hat{\boldsymbol{z}}\right\} \tag{11}$$

(we switch between spherical and Cartesian coordinates, using whichever coordinate system most clearly illuminates the physical phenomena). Integration of this force over the sphere volume gives a net force of $-2qB/3\hat{\boldsymbol{y}}$. One might expect the force on the dipole itself to be $qB\hat{\boldsymbol{y}}$. In a more careful examination of this problem, however, we replace the point dipole by a small sphere with a uniform "impressed" current density sufficient to produce a dipole moment q. In that case, one-third of the Ohmic return current flows through the small sphere ("within" the dipole), so the net force on the dipole is $2qB/3\hat{\boldsymbol{y}}$ and the net force on the entire system is zero[3] (this result is analogous to the demagnetizing field within a uniformly magnetized sphere [5]). The displacement and pressure fields are

$$\boldsymbol{u}=\frac{qB}{4\pi Gr}\left[\frac{3}{2}\left(1-\frac{r}{a}\right)\sin\theta\sin\phi\,\hat{\boldsymbol{r}}+\left(1-\frac{3r}{2a}\right)\cos\theta\sin\phi\,\hat{\boldsymbol{\theta}}+\frac{1}{2}\left(1-3\frac{r}{a}+\cos^2\theta\right)\cos\phi\,\hat{\boldsymbol{\phi}}\right] \tag{12}$$

$$p=\frac{qB}{2\pi r^2}\left[1-\left(\frac{r}{a}\right)^3\right]\sin\theta\sin\phi. \tag{13}$$

The radial displacement and the pressure vanish at the sphere surface; the shape of the sphere is not distorted. A schematic diagram of the displacement field is shown in Fig. 1(c). Again, there is no net force or torque on the sphere, only shear. Comparing (9) and (12), we see that the magnitude of the surface displacement is similar (on the order of $qB/4\pi Ga$) whether the dipole is perpendicular or parallel to the dipole; only its spatial distribution is affected significantly.

These two examples are special cases, but some of the conclusions hold generally. For instance, the net force, $\boldsymbol{F}$, on a tissue is equal to $\boldsymbol{J}\times\boldsymbol{B}$ integrated over the tissue volume. If the applied magnetic field is uniform, then

$$\boldsymbol{F}=\int\boldsymbol{J}\times\boldsymbol{B}\,dV=\int\boldsymbol{J}\,dV\times\boldsymbol{B}, \tag{14}$$

and it can be shown that for any current density that is entirely within a bounded tissue and has zero divergence, $\int\boldsymbol{J}\,dV$ is zero. In this case, there will be no net force on the tissue. There would, however, be a net force if the applied magnetic field has gradients. In general, if the action currents produce a net magnetic moment there will be a net force in a nonuniform magnetic field; there will also be a net torque on the tissue in either a uniform or nonuniform magnetic field. In the above example, the net magnetic moment is zero by the special symmetry, so that no torque results. Dimensional analysis indicates that the displacement should scale as qB/Gd and pressure should scale as qB/d^2, where d is characteristic of the distance between the source and detector. It is not clear from our results whether the sphere surface would be distorted by a dipole placed arbitrarily within the sphere; we see no reason to think that the surface would not distort in the general case.

IV. Eddy Currents

If the applied magnetic field is changing as a function of time, then eddy currents are induced in the tissue that could be as large as the bioelectric action currents.[4] These eddy currents could produce artifacts in the magneto-acoustic image. To appreciate their effect on the displacement and pressure distributions, we consider a conducting, elastic sphere in a uniform, time-dependent magnetic field. A conducting sphere is not an accurate model for a body, and inhomogeneities might significantly affect the eddy current distribution. The homogeneous sphere, however, provides a simple first approximation upon which more elaborate calculations can be based.

The eddy currents are governed by Faraday's law, $\nabla\times\boldsymbol{E}=-\partial\boldsymbol{B}/\partial t$, and Ohm's law, $\boldsymbol{J}=\sigma\boldsymbol{E}$, where σ is the conductivity of the sphere and $\boldsymbol{E}$ is the induced electric field. The current density induced in the sphere is

$$\boldsymbol{J}=-\frac{\sigma r\sin\theta}{2}\frac{\partial B}{\partial t}\hat{\boldsymbol{\phi}}. \tag{15}$$

If the magnetic field is oscillating as $\sin(\omega t)$, where ω is the angular frequency, the Lorentz body force is

$$\boldsymbol{J}\times\boldsymbol{B}=-\frac{\sigma}{2}\omega B^2 r\sin\theta[\hat{\boldsymbol{r}}\sin\theta+\hat{\boldsymbol{\theta}}\cos\theta]\cdot\sin(\omega t)\cos(\omega t). \tag{16}$$

It is straightforward to verify that the displacement and pressure fields are

$$\boldsymbol{u}=\frac{\sigma}{84G}\omega B^2 r^3[(1-3\cos^2\theta)\hat{\boldsymbol{r}}+5\sin\theta\cos\theta\,\hat{\boldsymbol{\theta}}]\cdot\sin(\omega t)\cos(\omega t) \tag{17}$$

$$p=\frac{(a^2-r^2)\sigma}{6}\omega B^2\sin(\omega t)\cos(\omega t). \tag{18}$$

There is a nonvanishing radial displacement at the sphere surface, which deforms the sphere into an ellipsoid. This result is analogous to the displacement field produced by a rotating sphere; e.g., the effect of earth's rotation on its shape [14]. At a given frequency, the force on the eddy currents increases as

[3] Replacing the point dipole by a finite radius sphere also eliminates the singularity of the displacement and pressure fields at the origin.

[4] Recall that we assume the skin depth is large compared to the tissue size, so that the magnetic field produced by the eddy currents is small compared to the applied magnetic field, and depth-dependent phase shifts can be neglected.

the square of the magnetic field strength, whereas the force on the action currents increases linearly with field strength, so that eddy current artifacts might be eliminated by performing experiments at several magnetic field strengths and subtracting from the data the part that varies as field strength squared. What is more important is that if the applied magnetic field varies sinusoidally, the pressure resulting from eddy currents will have twice the frequency of the applied magnetic field $[\sin(2\omega t) = 2\sin(\omega t)\cos(\omega t)]$. If a lock-in amplifier is used to detect the component of the pressure signal oscillating at the same frequency as the applied magnetic field [1], then eddy current artifacts are eliminated as long as the displacement transducer has a linear response.

V. Interpreting Experiments in a Tissue Bath

So far, we have considered the displacement and pressure fields in an elastic solid. Many of the preliminary magneto-acoustic experiments, however, were performed in a tissue bath, which is better modeled as a fluid than a solid. If we consider the Navier–Stokes equation for fluid dynamics [15], we obtain

$$\rho\frac{\partial \boldsymbol{v}}{\partial t} + (\boldsymbol{v}\cdot\nabla)\boldsymbol{v} = \eta\nabla^2\boldsymbol{v} - \nabla p + \boldsymbol{J}\times\boldsymbol{B} \qquad (19)$$

where $\boldsymbol{v}$ is the fluid velocity and η is the viscosity.[5] For the case of a dipole located at the center of a fluid sphere and oriented parallel to the magnetic field, symmetry considerations dictate that the nonlinear term in (19) vanishes, so for steady flow the Navier–Stokes equation reduces to (2) with $\boldsymbol{v}$ and η replacing $\boldsymbol{u}$ and G. Determining the velocity field for a dipole perpendicular to the magnetic field requires solving the full nonlinear Navier–Stokes equation, so the solution may differ considerably from the corresponding linear elasticity problem.

Soft tissue is neither a fluid nor an elastic solid, but a continuum having both fluid and solid constituents. A more appropriate model of soft-tissue is a poroelastic medium [11]. A poroelastic network behaves much like an incompressible elastic solid over times that are short compared to the consolidation time constant, which is on the order of seconds [11].

VI. Analogy between Magneto-Acoustic and Biomagnetic Imaging

There is a remarkable analogy between magneto-acoustic and biomagnetic current imaging. Taking the curl of Ampere's law governing the biomagnetic field produced by action currents, $\nabla\times\boldsymbol{b} = \mu_0\boldsymbol{J}$, we find that

$$\nabla^2\boldsymbol{b} = -\mu_0\nabla\times\boldsymbol{J} \qquad (20)$$

where μ_0 is the permeability of free space. Equations (4) and (20) describe the magneto-acoustic pressure and the biomagnetic field at an arbitrary location in an unbounded sample. Magneto-acoustic pressure recordings and biomagnetic measurements image action currents in an equivalent way: they both have $\nabla\times\boldsymbol{J}$ as their source, and are related by

$$p = \frac{1}{\mu_0}\boldsymbol{b}\cdot\boldsymbol{B}. \qquad (21)$$

This result is reminiscent of the "magnetic pressure" that arises in the equations of magnetohydrodynamics [5]. The similarity of (4) and (20) allow us to apply much of what is known about biomagnetic measurements to magneto-acoustical imaging. In biomagnetic models, action currents are often divided into non-Ohmic sources and Ohmic volume currents. Since a quasistatic electric field has zero curl, the Ohmic volume currents contribute to the magneto-acoustic or biomagnetic source only if the volume conductor is bounded, electrically inhomogeneous, or anisotropic. If we model an isotropic conductor as being piecewise homogeneous, then $\nabla\times\boldsymbol{J}$ is nonzero only at the boundary between regions of differing conductivity, where secondary sources may arise; a surface that is perpendicular to the applied magnetic field creates no secondary sources of pressure. Analogously, the component of the biomagnetic field that is perpendicular to a surface contains no contribution from any secondary sources on that surface. Because magneto-acoustic pressure measurements and biomagnetic techniques provide similar information about the current distribution, their relative usefulness depends on practical considerations such as cost, invasiveness, spatial resolution, and signal-to-noise ratio. Both methods require solving a nonunique inverse problem to obtain information about the current sources from quantities measured outside of, or on the surface of, the tissue. While we will not pursue it in this paper, it should also be possible to extend the analogy by describing the measurements of both pressure and biomagnetic fields in terms of the lead fields of the associated sensors [13].

A dipole centered in a sphere produces no external biomagnetic field, but does produce a surface displacement when it is parallel to an applied magnetic field. In this case, more information about the current source is available from magneto-acoustic imaging than from biomagnetic measurements. This additional information arises in part because of the shear displacements that are produced in response to current gradients parallel to the applied magnetic field (6), which have no analogy in biomagnetic imaging.

VII. Discussion

Based on our discussion so far, and the experimental work by Towe [1]–[4], magneto-acoustic imaging may appear to be an attractive alternative to other methods for studying action currents. This optimism is tempered when we calculate the actual pressures and displacements that arise during imaging. For a dipole at the center of an elastic sphere, the displacements at the sphere surface are on the order of $qB/(4\pi Ga)$. When we substitute reasonable values for these parameters we can estimate the surface displacements. A dipole moment of $1\,\mu$A m is typical of cardiac equivalent dipoles; other current sources would probably be smaller than this. The shear modulus for soft tissues are on the order of 10^4 N/m^2 [11]. If we assume the sphere has a radius of 1 cm (most bodies would be larger,

[5] For steady, low Reynolds number flow (when viscous forces dominate inertial forces), (19) has the same form as Navier's equation (2), with the velocity taking the place of the displacement, and the viscosity taking the place of the shear modulus.

but smaller bodies have larger displacements, and we wish to examine an optimistic case), and if this sphere is placed in a magnetic field of 1 T, the resulting surface displacements are about 1 nm. If the dipole is perpendicular to the magnetic field, the pressure produced in the sphere is on the order of $qB/(2\pi r^2)$, or about 1/6 N/m^2 ($1/6\times10^{-5}$ atm) at 1 mm from the sphere center. If the imaging experiments are performed in a tissue bath,[6] where (21) holds, then the fluid velocities on the sample surface are approximately $qB/(4\pi\eta a)$. The viscosity, η, for water is about 10^{-3} N s/m^2. Using the same parameters as above, the surface velocities would be about 0.01 m/s.

These tiny pressures and displacements demonstrate that great care is required to observe the magneto-acoustic effect. Towe's initial work [1] was performed by applying current to a tissue and measuring the net force. Since current was applied externally, the conclusions above, requiring that the net force be zero, no longer hold. It is not clear how well these experiments relate to the more interesting application of imaging endogenous bioelectric current. Our theoretical predictions indicate that magneto-acoustic imaging of endogenous bioelectric currents might be significantly more difficult to achieve than might be inferred from the experiments reported to date.

One limitation of our model of magneto-acoustic imaging is that we have neglected acoustic wave propagation. Propagation effects need to be included for quantitative analysis of the high frequency components of the recorded displacement or pressure. Interestingly, the possibility exists for acoustic resonances at high frequencies, resulting in relatively large amplitude standing waves that might be particularly sensitive to the geometry of the object being imaged or the fluid-filled container that might be holding it. Nevertheless, the low-frequency, or near-field, approximation should be valid for many biomedical applications. Indeed, the near field approximation we present should be significantly more accurate than the far field approximation adopted by Islam and Towe [2] in their image reconstructions from magneto-acoustic measurements.

We showed that when the applied magnetic field is oscillating, artifacts introduced by eddy currents can be removed by filtering the pressure or displacement signals. Nevertheless, it is instructive to calculate how big these effects are. The surface displacements on a 1 cm radius sphere with a conductivity of 1 S/m and a shear modulus of 10^4 N/m^2 placed in a 1 T magnetic field oscillating at a frequency of 1 kHz are about 10 nm (we realize that creating a 1 T, 1 kHz magnetic field for large samples would be quite a technological feat; surface displacements would likely be smaller in any real macroscopic imaging system). This displacement is small compared to the sphere radius, but is about an order of magnitude larger than the displacement estimated for action currents. In a larger sample, the eddy current displacements are larger, whereas the displacements due to action currents get smaller, making the potential for eddy current artifacts even greater.

Even with the small displacements and pressures involved, it is possible that magneto-acoustic imaging could be used to image bioelectric action currents both *in vivo* and *in vitro*. We note, however, that there are several limitations to this technique. For imaging action currents *in vivo*, the sounds produced by the magneto-acoustic mechanism might be overwhelmed by the ambient noise, e.g., sounds produced by muscle contraction, and fluid or gas movement. These artifacts might be reduced by using an applied magnetic field that oscillates at a higher frequency (on the order of 1 kHz) than these body sounds [4]. The magneto-acoustic technique may have promise for *in vitro* experiments, but even an isolated nerve in a bath produces sounds that are not of magneto-acoustic origin. For example, there is a rapid volume expansion caused by impulse conduction in unmyelinated nerve fibers even when no magnetic field is present, which can cause pressure changes on the order of 10^{-6} atm in a closed, water-tight nerve chamber [16]. Using an oscillating applied magnetic field and a lock-in amplifier to detect the magneto-acoustically induced pressure distribution might overcome these difficulties [1].

One attractive application of magneto-acoustic imaging might be for microscopic samples (1 mm^3 volume or less). In our earlier example of a dipole in a sphere, the surface displacements produced by a dipole increase as the sphere radius is decreased, but the artifacts produced by eddy currents decrease with the sphere radius. Making the sample smaller, therefore, increases the desired signal (bioelectric activity) relative to artifact (eddy currents). Because a sample is small, limitations from the skin depth are minimized, so higher frequencies (possibly in the megahertz region) might be used, if desired. Moreover, the engineering constraints for producing strong, rapidly changing magnetic fields are less significant for microscopic samples. Microscopic magneto-acoustic imaging might, therefore, have technological advantages over magneto-acoustic imaging of macroscopic samples. Possible applications include the detection of injury currents in damaged nerves and skeletal muscle or ischemic cardiac tissue, the detection of wavefronts of spreading depression in the cerebral cortex currents, and imaging of current in oocytes and other developing cells and cell systems. It remains to be demonstrated whether the technique has the requisite sensitivity and spatial resolution for such measurements.

The method of magneto-acoustic imaging that we have described requires placing the tissue in a uniform magnetic field and detecting the acoustic signal at many locations on the tissue surface. This is, however, not the only way which imaging can be performed. Towe suggested using strong, localized magnetic fields from a magnetic recording head that could be scanned over a thin tissue slice, creating a scanning current microscope [4]. More generally, we might improve action current localization in any application of magneto-acoustic imaging by employing a method similar to one developed for estimating the anisotropic diffusion tensor with NMR [17]. Measurements of pressure or displacement could be made using magnetic field gradients applied along various

[6] Clearly an accurate model of an experiment in a tissue bath would require a somewhat different analysis, since the fluid would have to be contained, which would mean, on at least several sides the pressure would not necessarily be zero at the fluid surface, but the fluid velocity would. Our analysis, therefore, provides only an order-of-magnitude estimate of the fluid velocities one might expect.

oblique directions, so that each measurement weights the action currents in different regions within the tissue differently. This additional information would constrain the solution to the ill-conditioned inverse problem of determining the action current from the measured pressure or displacement fields. This feature of magneto-acoustic imaging has no analogy in biomagnetism, and may represent a significant advantage of magneto-acoustic methods over biomagnetic techniques.

When the applied magnetic field is not uniform in space, additional forces could arise due to inhomogeneities in magnetic susceptibility [18], [19]. These forces could produce artifacts in any algorithm for magneto-acoustic imaging of action currents that requires applied magnetic field gradients. We can turn this disadvantage around, however, and consider magneto-acoustic methods for imaging magnetic susceptibility, χ [19]. In this case, the force per unit volume on the tissue is not $\boldsymbol{J} \times \boldsymbol{B}$, but rather $\chi/\mu(\boldsymbol{B} \cdot \nabla)\boldsymbol{B}$. One possible biological application might be imaging susceptibility changes arising from changes in blood oxygenation, as is performed in functional magnetic resonance imaging [20]. Tomographic techniques with differing fields and gradients being applied from various directions should also be applicable [21].

REFERENCES

[1] B. C. Towe and M. R. Islam, "A magneto-acoustic method for the noninvasive measurement of bioelectric currents," *IEEE Trans. Biomed. Eng.*, vol. 35, pp. 892–894, 1988.

[2] M. R. Islam and B. C. Towe, "Bioelectric current image reconstruction from magneto-acoustic measurements," *IEEE Trans. Med. Imag.*, vol. 7, pp. 386–391, 1988.

[3] B. C. Towe, "Possibility of detecting nerve action currents by Lorentz force evoked sound waves," *J. Biomed. Eng.*, submitted for publication.

[4] B. C. Towe, "Possibility of imaging low-level bioelectricity by a Lorentz force method," *IEEE Trans. Biomed. Eng.*, submitted for publication.

[5] J. R. Reitz, F. J. Milford, and R. W. Christy, *Foundations of Electromagnetic Theory*. Reading, MA: Addison-Wesley, 1980.

[6] J. P. Wikswo, Jr., J. P. Barach, and J. A. Freeman, "Magnetic field of a nerve impulse: First measurement," *Science*, vol. 208, pp. 53–55, 1980.

[7] J. P. Wikswo, Jr. and J. P. Barach, "An estimate of the steady magnetic field strength required to influence nerve conduction," *IEEE Trans. Biomed. Eng.*, vol. BME-27, pp. 722–723, 1980.

[8] K. R. Swinney and J. P. Wikswo, Jr., "A calculation of the magnetic field of a nerve action potential," *Biophys. J.*, vol. 32, pp. 719–732, 1980.

[9] R. Plonsey and D. Heppner, "Considerations of quasi-stationarity in electrophysiological systems," *Bull. Math. Biophys.*, vol. 29, pp. 657–664, 1967.

[10] Y. C. Fung, *Foundations of Solid Mechanics*. Englewood Cliffs, NJ: Prentice-Hall, 1965.

[11] P. J. Basser, "Interstitial pressure, volume, and flow during infusion into brain tissue," *Microvasc. Res.*, vol. 44, pp. 143–165, 1992.

[12] Y. C. Fung, *Biomechanics*. New York: Springer-Verlag, 1990.

[13] J. P. Wikswo, J. A. V. Malmivuo, W. H. Barry, M. C. Leifer, and W. M. Fairbank, "The theory and application of magnetocardiology," *Adv. Cardiovasc. Phys.*, vol. 2, pp. 1-67, 1979.

[14] A. E. H. Love, *A Treatise on the Mathematical Theory of Elasticity*. New York: Dover, 1944.

[15] W.-H. Li and S.-H. Lam, *Principles of Fluid Mechanics*. Reading, MA: Addison-Wesley, 1976.

[16] I. Tasaki and P. M. Byrne, "Volume expansion of nonmyelinated nerve fibers during impulse conduction," *Biophys. J.*, vol. 57, pp. 633–635, 1990.

[17] P. J. Basser, J. Mattiello, and D. LeBihan, "Estimation of the effective self-diffusion tensor from the NMR spin-echo," *J. Magn. Res.*, ser. B, vol. 103, pp. 247–254, 1994.

[18] J. P. Wikswo, Jr., "Noninvasive magnetic detection of cardiac mechanical activity: Theory," *Med. Phys.*, vol. 7, pp. 297–306, 1980.

[19] J. P. Wikswo, Jr., Y. P. Ma, N. G. Sepulveda, S. Tan, I. M. Thomas, and A. Lauder, "Magnetic susceptibility imaging for nondestructive evaluation," *IEEE Trans. Appl. Superconductivity*, vol. 3, pp. 1995–2002, 1993.

[20] R. Turner, D. LeBihan, C. T. W. Moonen, D. Despres, and J. Frank, "Echo-planar time course MRI of cat brain oxygenation changes," *Magn. Reson. Med.*, vol. 22, pp. 159–166, 1991.

[21] N. G. Sepulveda, I. M. Thomas, and J. P. Wikswo, Jr., "Magnetic susceptibility tomography for three-dimensional imaging of diamagnetic and paramagnetic objects," *IEEE Trans. Magn.*, in press.

Bradley J. Roth received the Ph.D. degree in physics from Vanderbilt University, Nashville, TN. He attended Vanderbilt on a National Science Foundation Graduate Fellowship. His graduate research was performed in the Living State Physics Laboratory, and resulted in the first detailed comparison of the transmembrane potential and magnetic field produced by an isolated nerve axon, and the prediction of electrically silent magnetic fields generated by electrical activity at the apex of the heart.

After obtaining the Ph.D. in 1987, he remained at Vanderbilt for one year as an American Heart Association–Tennessee Affiliate Research Fellow, during which time he developed Fourier methods for solving the magnetic inverse problem with two-dimensional current sources. He is presently a Senior Staff Fellow with the Biomedical Engineering and Instrumentation Program at the National Institutes of Health.

Peter J. Basser was born in New York in 1957. He received the S.M. and Ph.D. degrees in engineering sciences from Harvard University in 1982 and 1986, respectively.

He is presently a Biomedical Engineer in the Mechanical Engineering Section of the Biomedical Engineering and Instrumentation Program, National Institutes of Health, Bethesda, MD. His current research interests include developing noninvasive methods to stimulate excitable tissues and measure their physical properties, as well as continuum models to describe coupled transport processes in tissue and gels.

John P. Wikswo, Jr. was born in Lynchburg, VA in 1949, and graduated from Amherst County High School in 1966. He received the B.A. degree in physics from the University of Virginia in 1970, and the M.S. and Ph.D. degrees in physics from Stanford in 1973 and 1975, respectively.

He was a Research Fellow in Cardiology at the Stanford University School of Medicine from 1975 to 1977, where he continued his work on determining the relationship of the electric and magnetic fields of the heart and developing instrumentation and analysis techniques for magnetocardiography. He joined the faculty in the Department of Physics and Astronomy at Vanderbilt University as an Assistant Professor of Physics in 1977. He is now the A.B. Learned Professor of Living State Physics. He is a fellow of the American Physical Society. His current research is directed towards using electric and magnetic measurements and electromagnetic theory for studying the propagation of electrical activity in nerve and muscle cells and for nondestructive testing. He has published over 70 research articles and book chapters, and more than 150 conference papers, abstracts, and reports. He holds five patents.